The LEGO theory of the developing functional connectome

Erica L. Busch[1†], Kristina M. Rapuano[1], Kevin Anderson[1], Monica D. Rosenberg[2], Richard Watts[1], BJ Casey[1], James Haxby[3], Ma Feilong[3†]

[1]Department of Psychology, Yale University
[2]Department of Psychology, University of Chicago
[3]Department of Psychological and Brain Sciences, Dartmouth College

[†]Corresponding authors:
Erica L. Busch: Erica.Busch@yale.edu
Ma Feilong: mafeilong@gmail.com

Abstract

Decades of human magnetic resonance imaging (MRI) research demonstrate that variance in neuroimaging phenotypes, including functional connectivity, relate to genetics[1–5] and predict cognitive traits[6–9]. The functional connectome affords information transmission through the brain at various spatial scales, from global oscillations between broad cortical regions to fine-scale connections that underlie specific information processing[10,11]. In adults, while both the coarse- and fine-scale functional connectomes predict cognition[6,12–14], the fine-scale connectome predicts twice as much cognitive variance[15]. Yet, past brain-wide association studies, particularly using large developmental samples, have limited their focus to the coarse connectome to understand the neural underpinnings of individual differences in cognition[8,9,16–18]. We studied resting-state fMRI in 1,115 children (including 389 twin pairs) and used functional alignment to afford access to individual differences in the fine-scale connectome[10,19,20]. We found that even though individual differences in the fine-scale connectome are more reliable than those in the coarse-scale connectome, they are less heritable. This surprising result indicates that genetically-determined versus experience-dependent factors in brain development have dissociable effects on these two spatial scales of the connectome. We show further that both connectome scales equally predict a more heritable trait (general cognitive ability) in childhood, but only the fine scale effectively predicts a more experience-driven trait (learning/memory). As such, the developing functional connectome resembles a LEGO® set: the specific pieces a child has parameterizes what they will eventually build, but even when given identical sets, two children with unique experiences will build different creations.

Introduction

The building blocks of the functional connectome are an interplay of genetics[5,21,22] and experience[1,23]. Functional connections at various spatial scales, ranging from coarse, global regional oscillations to vertex-wise patterns of information transfer, account for related, yet different, types of information encoding and transmission[10,11]. While variation in functional connectivity can predict individual differences in aspects of memory[12], attention[13], and intelligence[15], among other cognitive traits[8,14,24,25], it is unclear how the spatial scales of functional connectomes differentially contribute to genetic and experience-based cognitive traits during periods of biological and experiential maturation. To understand how this is reflected at the population level in the developing brain will require consideration of how we define functional connectivity information at both fine and coarse scales. In the current study, we disentangle experience-based idiosyncrasies in the functional connectome from genetic influences by estimating the heritability, reliability, and predictive validity of resting-state functional connectivity (RSFC) based on connectome granularity during development[26,27].

Structural and functional magnetic resonance imaging (MRI) of twin samples reveal strong genetic control over various measures of brain morphology[1–3,28,29] and RSFC[21,22,30–34]. RSFC is a powerful tool for investigating individual differences in brain–behavioral associations, especially in clinical and developmental populations where task-based fMRI is often difficult[8,24,25,35]. Genetic influences on brain structure and function increase with age[2,36], are associated with cognitive functioning[2], and interact with the environment to sculpt an individual's functional connectome[2,5,36,37]. Structural MRI, which is used to derive anatomical alignment of functional imaging data across subjects, has been demonstrated to have limited reliability in large-scale

developmental neuroimaging studies, which impacts the reliability of aligning data across developing brains using structural brain images alone[16].

Recent studies looking at the genetic control over RSFC have focused on traditional functional connectivity calculations, such as the coupling of specific regions of interest[38] , or oscillations between brain networks using group parcellations[21,22] or, more recently, individualized atlases[32]. Dividing the cortex into subfields and collapsing over the hundreds of cortical vertices within a predefined neuroanatomical region can mitigate high-dimensionality, measurement instabilities, and idiosyncratic cortical functional organization. However, recent adult studies have shown that vertex-wise functional connectivity across the cortex ("fine-scale connectomes") better reflect reliable individual differences in functional connectivity[39] and capture twice as much variance in cognitive ability (e.g., intelligence)[15] than group-average parcellations ("coarse-scale connectomes"). To what extent are the fine-scale patterns of functional connectivity under genetic control, and would accessing this connectome tighten the link between functional connectivity, cognition, and genetics? Or is there a dissociation of genetic control over these two scales of connectivity? Here we use novel machine learning approaches to relate connectome granularity and estimates of heritability, reliability, and predictions of neurocognitive ability during development (Figure 1). Specifically, we use connectivity hyperalignment[19] to access functional information processing in the fine-scale connectome, and tease it apart from the coarse-scale connectome which reflects less-specific fluctuations across broad swaths of cortex.

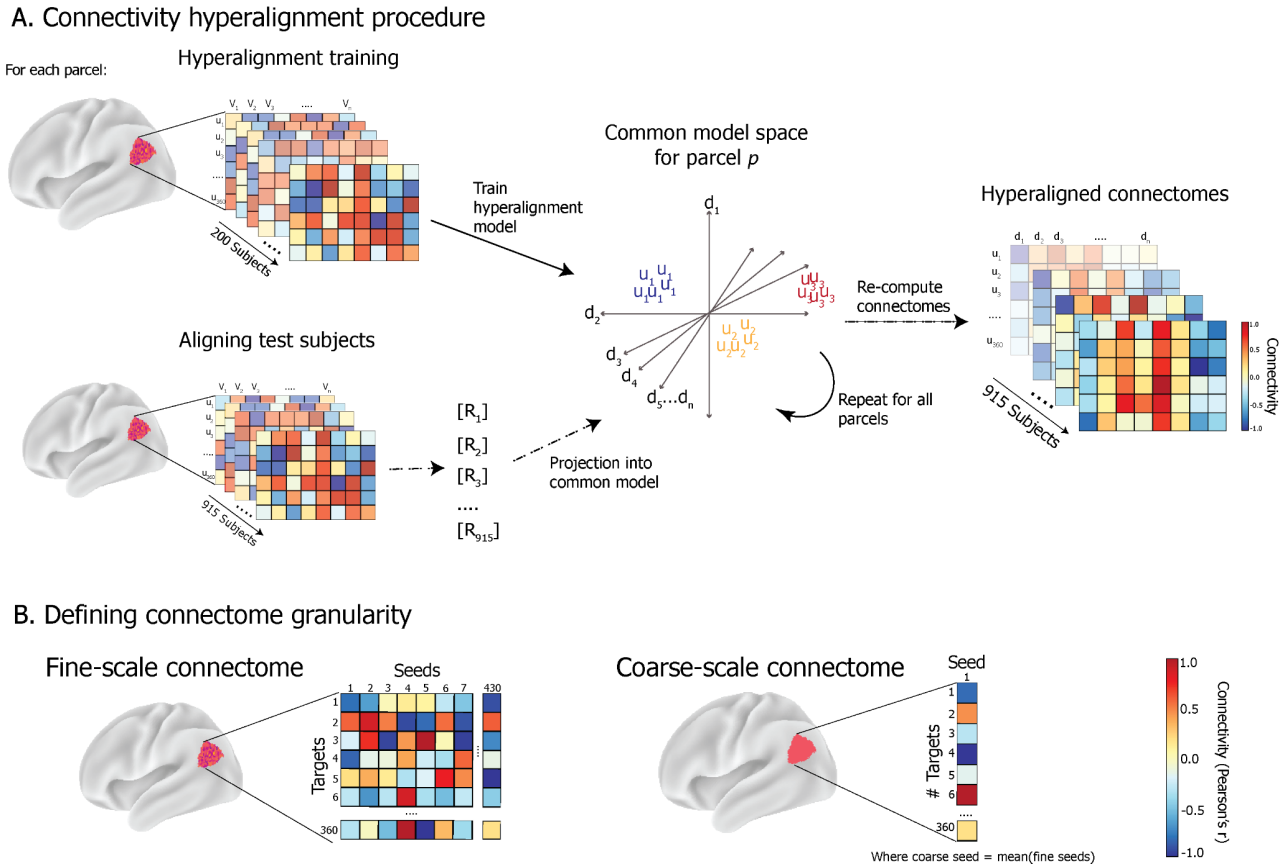

Figure 1: Methods

A. Connectivity hyperalignment training procedure. For each parcel in the Glasser parcellation (here, region 329 with 430 cortical vertices), connectivity matrices are computed as the strength of connection (Pearson's correlation) between the activity timeseries of vertices within the parcel (seeds; *u*) and the average activation across vertices in all other parcels (targets; *v*). The connectivity matrices for 200 held-out subjects are used to train the hyperalignment common model space for a given parcel. The model space is of dimensions $\mathbf{D} = [d_1 \ldots d_n]$ which are weighted combinations of $\mathbf{U} = [u_1 \ldots u_n]$, the dimensions of each subjects' connectivity matrices in anatomical space. **D** represents the space where connectivity targets are best aligned across training subjects. Then, connectomes for the 915 test subjects are projected into **D** via subject-specific transformation matrices **R**, which detail a mapping from given subject *i's* anatomical space $\mathbf{U_i}$ into **D.** This procedure is repeated to derive **R** for each test subject and parcel. Then, the regional activation pattern for each parcel in anatomical space is mapped via **R** into the region's common space to compute the hyperaligned timeseries for each subject, which is then used to recompute connectivity matrices between hyperaligned seeds *v* and model dimensions *d.* **B. Connectome granularity.** Fine-scale connectomes are multivariate patterns of the connectivity weights between all vertices in a given parcel and the average pattern of each other parcel in the brain. Coarse-scale connectomes are vectors (univariate), representing the

connectivity weight between the average pattern of a given parcel and those of each other parcel in the brain.

Results

Establishing reliable connectomes

Variability in RSFC can reflect idiosyncrasies driven by cortical communication patterns indicative of neurocognitive variability, but it can also reflect artifacts due to data acquisition noise, movement, and functional–anatomical mismatch. In adult populations, brain parcellations (e.g. Glasser parcellation[40]) average adjacent areas of cortex to improve signal-to-noise and reduce the dimensionality of the data. This approach assumes functional–anatomical correspondence will improve at the group level and comes at the cost of lower granularity.

Here, we analyze RSFC between subjects (see Table S1 for subject breakdown) using two methods of group alignment. The first uses a standard approach to align data in a common space based on anatomical location (anatomical alignment [AA]), while the second approach uses connectivity hyperalignment (CHA)[19] to learn a representational space based on common patterns of functional connectivity via an adapted Generalized Procrustes Analysis (see Methods for details). CHA allows for local remixing of vertex-wise functional connectivity patterns within an anatomically-constrained region[20], thereby aligning common patterns of fine-scale information within broader regions of interest by removing idiosyncrasies caused by noise or functional–anatomical correspondence[10]. In contrast with coarse alignment, which averages across the region and can diminish differences across subjects, CHA affords fine-scale functional alignment: projecting all of the region's information patterns into high-dimensional common space to align information across subjects based on *functional* instead of *anatomical* information

topographies (Figure 1B). Within this common space, individual differences in functional connectivity become more pronounced and reliable[39], particularly at the fine-scale representational level, and are better predictive of cognitive traits[15] in adults. In contrast, previous studies have applied a reduced-dimensional hyperalignment algorithm (shared response model) to align child brain responses to an adult-defined common model as the two groups performed the same task[41]. To address the question of individual differences in fine-scale functional connectivity among children, we present (to our knowledge) the first derivation of a child-defined and applied model of shared brain function, which negates concerns about differences in cortical development or anatomy conflating functional connectivity patterns. We then address the relative effects of functional alignment versus simply higher-dimensional measurements by averaging the functionally-aligned CHA data and by retaining the high-dimensional, anatomically aligned data, to have a full comparison of AA coarse, AA fine, CHA coarse, and CHA fine-scale connectomes.

Our first analysis looks at the reliability of idiosyncrasies in functional connectivity patterns across connectome alignment and granularity. Here, idiosyncrasies are defined as how similar a subject's connectome is to their own connectome across split-halves, relative to their similarity to all other subjects. CHA, particularly at the fine scale, improves the reliability of functional connectivity over anatomical alignment alone (Figure 2). Across all parcels, reliability of coarse connectomes increased from an average of $r=0.34 \pm 0.1$ for AA to $r=0.58 \pm 0.08$ for CHA. Reliability of fine connectomes increased from an average of $r=0.43 \pm 0.11$ for AA to $r=0.86 \pm 0.07$ for CHA. After CHA, 100% of parcels at both scales showed greater reliability, and 99% of parcels showed greater reliability at the fine scale than the coarse scale. Notably, all four types of

connectomes show high split-half reliability, with CHA affording the greatest reliability. This establishes that hyperalignment improves access to reliable information within an individual's functional connectome, despite training the model on held-out subjects. Particularly at the fine scale, functional connectivity information is diagnostic of the individual[42], affording confidence that subsequent results using this information are driven by reliable individual differences as opposed to noise.

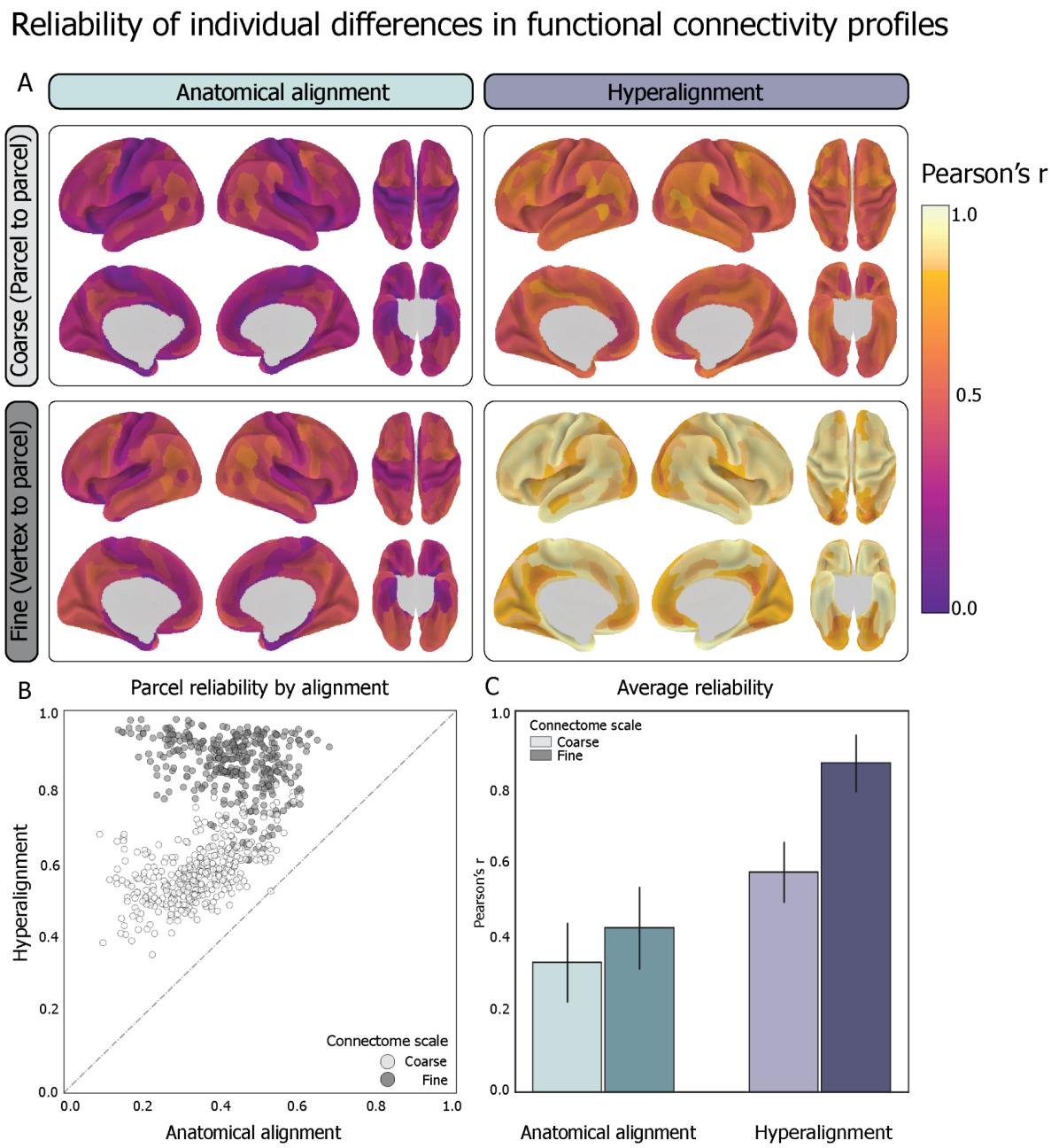

Figure 2. Reliability of individual differences in functional connectivity profiles

A. Procedure: The reliability of individual differences in functional connectivity profiles between regions (defined with the Glasser parcellation[40]) was analyzed with data from 526 unrelated subjects. Subjects' timeseries data for each parcel were split into two halves, which were hyperaligned into the trained common space separately. For each region, split timeseries data pre- and post-hyperalignment were used to compute functional connectivity profiles at the fine and coarse scales. Then individual dissimilarity matrices (IDMs) were computed across all pairs

of subjects. The IDMs for each split were then correlated (Pearson's r) to get a measure of the reliability of individual differences captured by the regional functional connectivity profiles, presented on the cortex for the coarse and fine scales before and after hyperalignment. This approach is a variation of the "fingerprinting"[14,42] approach, whereby measured individual differences are more reliable if a subject is more similar to themselves across split-halves than to any other subject. **B.** The reliability of individual differences increases after hyperalignment for all parcels. 99% of fine connectivity profiles (darker) are more reliable than coarse ones (lighter) regardless of alignment type. **C.** Bars presented as the average reliability (Pearson's r) across all parcels in the Glasser parcellation. Error bars represent ± standard deviation from the mean.

Genetic control over the coarse-scale connectome

Our reliability analysis revealed that the fine-scale connectome is more reliable within individuals than the coarse scale, and this is particularly salient after connectivity hyperalignment (HA). Given that the fine-scale CHA data reveal more reliable, idiosyncratic functional connectivity patterns than the coarse data, we hypothesized it would be less influenced by genetics. In other words, the broad anatomical alignment would reflect the heritability of cortical anatomy previously shown[1,36,37], but the functional alignment would disentangle the fine-scale functional differences in connectivity information, reflecting more reliable, behaviorally-informative individual differences driven by unique life experiences.

The heritability analysis used RSFC data from 778 subjects comprising 219 dizygotic twin pairs and 170 monozygotic twin pairs (see breakdown in Table S1). Functional connectomes of vertex-granularity are an inherently high-dimensional phenotype. To explicitly model the heritability of this phenotype, we used a multidimensional estimate of heritability[32] to model both the phenotypic similarity matrix between participants as well as the genetic kinship matrix (see *Multidimensional heritability estimate* for more information). As predicted, we find differential heritability according to the alignment and granularity of functional connectomes, where 99.6%

percent of parcels are more heritable at the coarse scale than the fine scale ($p<0.01$) (Figure 3). At the coarse scale, anatomically-aligned functional connectomes are significantly more heritable than hyperaligned connectomes (AA = 0.198 ± 0.05; CHA = 0.161 ± 0.04; $p < 0.01$), with 96% of parcels showing greater heritability. These results indicate that connectivity information aligned coarsely based on anatomical features are under strong genetic control, consistent with previous studies showing genetic control over cortical anatomy in children[28] and network-level RSFC[21].

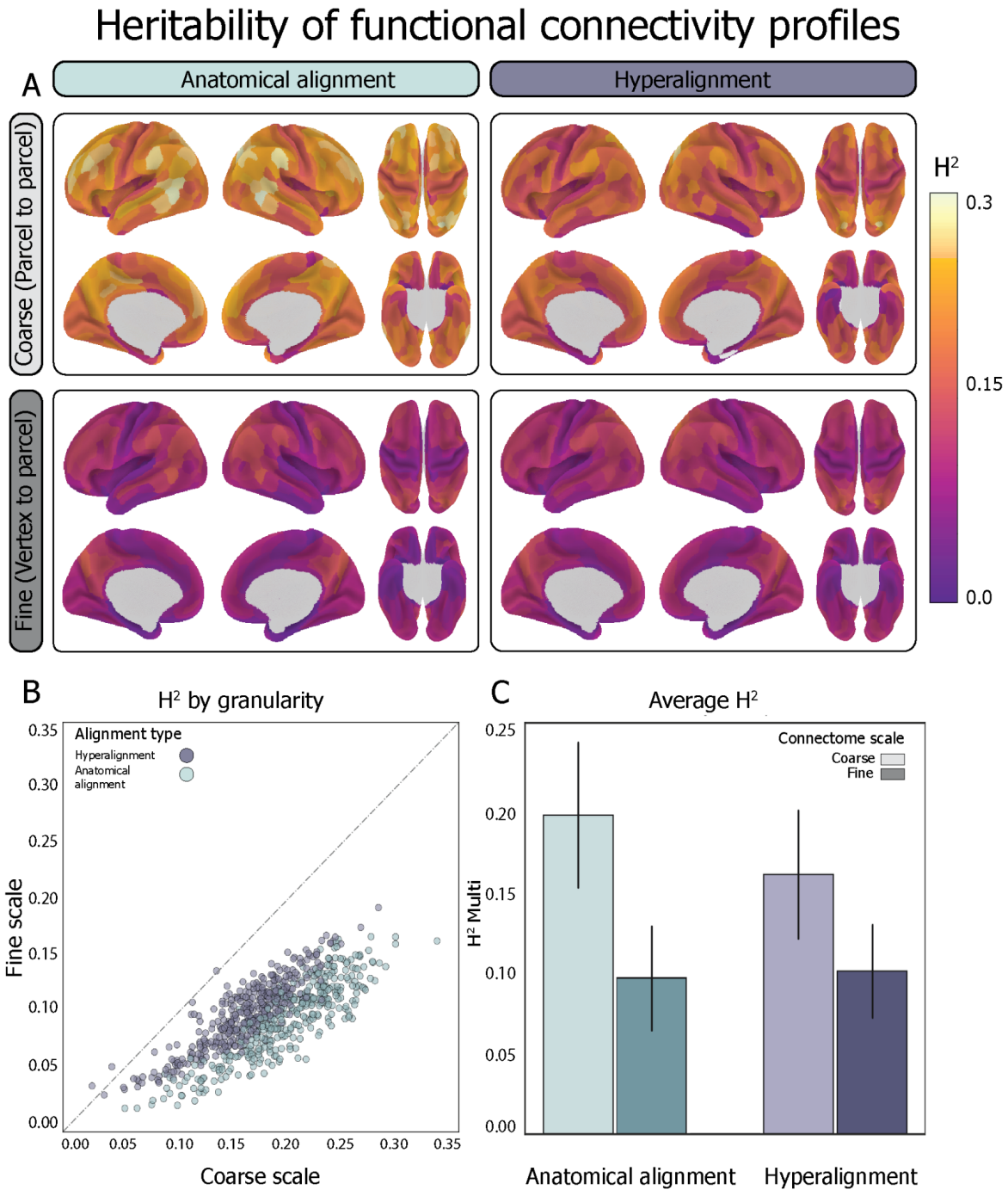

Figure 3. Heritability of functional connectivity profiles

A. Heritability of functional connectivity profiles between regions (defined with the Glasser parcellation[40]) was estimated using a multidimensional heritability model[32] using resting-state fMRI data from 778 9-10 year-olds (170 MZ pairs and 219 DZ pairs). Functional connectivity between a given parcel and all other parcels in the brain was calculated at fine and coarse granularities, before and after functional alignment. The coarse-grained connectivity profiles aligned based on cortical anatomy are the most heritable. **B.** For both anatomically-aligned and

hyperaligned data, connectivity profiles are more heritable when calculated at the coarse scale than the fine scale (99.6 percent of the time). **C.** At the coarse scale, the anatomically aligned connectivity profiles are more heritable than the hyperaligned ones; this distinction dissipates at the fine scale, which is under comparatively minuscule genetic control. Bars presented as the mean heritability across all parcels in the Glasser parcellation and error bars presented as standard deviation.

Prediction of neurocognitive abilities

Having established that the coarse, anatomically-aligned functional connectome is under strong genetic control and that all connectomes showed reliability, we sought to demonstrate their functional significance by teasing apart connectome granularity as it relates to heritability versus behaviorally-relevant idiosyncrasies. Compared with brain structure, complex psychological traits are less heritable, but cognitive abilities are among the most heritable dimensions of human behavior[43]. Heritability of these traits vary by cognitive domain with higher estimates reported for general cognitive ability (h^2 = .67–.80) than for learning/memory (h^2 = .36–.56)[44], which may be more sensitive to experiential factors. We leveraged this variation in heritability of cognitive traits to examine the functional significance of our heritability and reliability findings. General cognitive ability and learning/memory scores were defined based on previously reported principal components analysis of the NIH Toolbox tasks used in the ABCD study[45]. Because learning/memory is less heritable than general cognitive ability, we can compare variation in connectome heritability on prediction of cognitive phenotypes[44]. Since CHA improves reliability of individual differences in the fine-scale connectome, we expected CHA fine connectomes generally to be more predictive of cognitive performance (i.e., both general cognitive ability and learning/memory) than either CHA coarse, AA coarse or fine connectomes. Moreover, we expected the most heritable connectivity information (i.e., AA coarse) to better predict a more heritable cognitive ability (general ability) relative to a less heritable trait (learning/memory).

We used PCA ridge regression to predict scores on these two cognitive domains from connectivity profiles at each scale. Models were scored as R^2 between predicted scores and true scores using nested cross-validation (see Neurocognition PC prediction analysis for more details), and significance of R^2 values were assessed with permutation tests (10,000 iterations per model). Model scores were compared across connectome types using 10,000 bootstrap iterations with resampling.

Overall, hyperaligned fine-scale connectomes best predicted individual differences in cognitive performance (i.e., both general cognitive ability and learning and memory). As hypothesized, the degree to which the coarse connectome also contributed to prediction was associated with the heritability of the trait. General cognitive ability has high heritability for a psychological trait (h^2 = .67–.80)[44] and was similarly predicted by CHA fine, AA coarse, and AA fine connectomes (average parcel R^2 ± s.d. across parcels; CHA fine = 0.0133 ± 0.021; AA fine = 0.0134 ± 0.020; AA coarse = 0.0124 ± 0.018; CHA fine vs. AA fine $p = 0.30$; CHA fine vs. AA coarse $p = 0.23$; AA fine vs. AA coarse $p = 0.08$) (Figure 4). General cognitive ability was predicted with significantly lower accuracy by CHA coarse, suggesting that functionally aligning fine-scale information then smoothing over the functional information space actually diminishes the specificity of the information. After performing permutation tests at each parcel and thresholding at $p < 0.01$, 42%, 42.5%, 30.5%, and 43% of parcels predicted general cognitive ability significantly greater than chance at the AA coarse, AA fine, CHA coarse, and CHA fine scales respectively (Figure S2A).

Learning/memory is regarded as a less heritable psychological trait (h^2 = .36–.56)[44], so we hypothesized the heritable scaffolding of the connectome (AA coarse) would contribute less information to this prediction than to prediction of cognitive ability, and the trait would be predicted more strongly from the CHA fine connectome. As expected, prediction of learning/memory scores were significantly higher for the CHA fine connectome than for CHA coarse (CHA fine R^2 = 0.018 ± 0.012; CHA coarse R^2 = 0.011 ± 0.014; $p < 0.0001$), AA fine (0.008 ± 0.014; $p = 0.09$), or AA coarse (0.007 ± 0.014; $p < 0.0001$) (Figure 4). The gap in the percentage of parcels surviving our permutation test was also more pronounced for this trait; 30%, 33%, 39%, and 61% for AA coarse, AA fine, CHA coarse, and CHA fine.

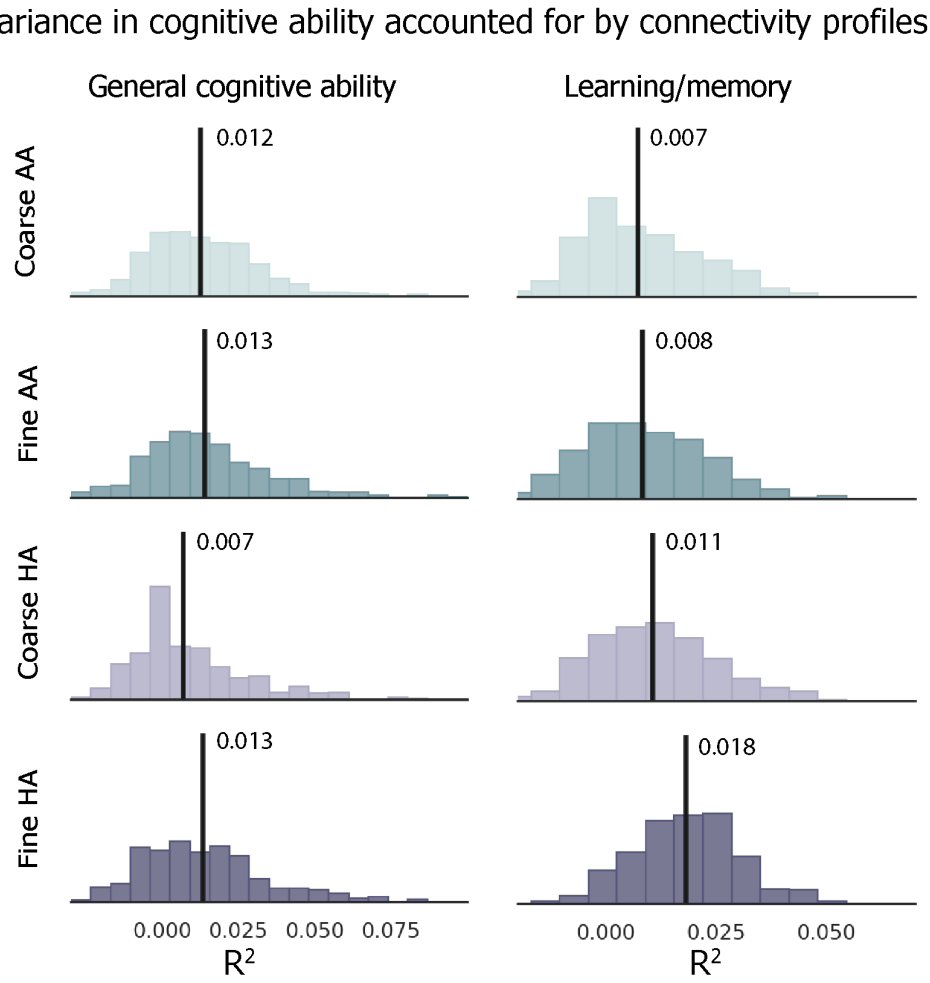

Figure 4: Prediction of neurocognitive PC loadings.
Distribution of R^2 values across all parcels for prediction of general cognitive ability (left) and learning/memory (right). Histogram heights correspond to density of scores and lines represent the mean of the score distribution. For the purpose of distribution matching, R^2 values are not thresholded here; thresholded R^2 values mapped to the cortical surface are displayed in **Figure S2**.

Discussion

In this study, we sought to understand how individual differences are realized at different spatial scales of the developing connectome, and how the variability captured by connectome granularity relates to genetic control and cognitive traits. Prior work indicates that both coarse

and fine-scale functional connectivity predicts idiosyncrasies in cognitive phenotypes in adults[12–15], and functional alignment (connectivity hyperalignment; CHA[19]) improves access to this variability in the fine-scale connectome[15,39]. Yet, to date, studies have related functional connectivity in youth to individual differences in cognition or behavior by looking only at coarse scale information. This spatial averaging reduces dimensionality and smooths idiosyncratic anatomy across subjects. Using CHA, we reveal reliably idiosyncratic patterns of fine-scale functional connectivity in the developing brain. The coarse-scale connectome (AA coarse) shows moderately reliable idiosyncrasies (mean Pearson's r=0.34), versus the CHA fine connectome's mean reliability of r=0.86 (Figure 2). Across the entire brain, individual differences in fine-scale connectivity are more reliable than in coarse-scale, indicating that the traditional coarse alignment approach diminishes the detailed, spatially-resolved topographies of information transfer in the developing brain.

By estimating the heritability of functional connectivity at each scale and alignment, we showed that idiosyncrasies in the fine-scale connectomes are dissociable from idiosyncrasies in the coarse scale connectome. Multiscale heritability analysis of coarse-scale, anatomically aligned connectomes attribute about 20% of variance to genetic relatedness, which converges with our expectations based on adult coarse RSFC estimates[21,22,32] and how neuroimaging phenotypes increase in heritability with age[1,3]. At the fine scale, our estimates drop to around 10% regardless of alignment technique, suggesting that at the fine scale, idiosyncrasies in connectivity are more related to experience than genetics.

Individual differences captured by variable connectome granularity revealed a dissociation between the spatial scales of heritable and reliable patterns of functional connectivity. Our final analysis showed that this dissociation is also relevant in prediction of cognitive traits. Whereas both the most reliably idiosyncratic (CHA fine) and most heritable (AA coarse) connectomes were comparably predictive of general cognitive ability, a canonically heritable cognitive trait, the most reliably idiosyncratic connectome (CHA fine) was best predictive of a less heritable cognitive trait (learning/memory). Past studies using RSFC at a coarse scale from the ABCD dataset were only able to predict general cognitive ability and not learning/memory scores[8]. By improving the reliability of our data and accessing finer-scale information with CHA, we uncovered patterns of functional connectivity predictive of a more nuanced, experience-related cognitive trait (learning/memory).

Taken together, the link demonstrated here between reliable, heritable, and predictive scales of functional connectivity reveals the importance of nuanced, multi-scale connectivity analyses for building a holistic theory of individual differences during development. Consistent with the interactive specialization framework of functional brain development, the development of the functional connectome is not solely determined by a blueprint, but the interaction of a heritable template and individualized experience[46]. We present a novel approach to prediction of developing cognitive abilities from functional connectivity measured in different topographical representation spaces, by aligning information across brains based on functional alignment at high spatial resolution versus the traditional approach of coarse alignment (an adult-defined cortical atlas with averaging). Our study presents the first example of defining and applying a functional common space to a developmental cohort, negating the very issues that arise with

developmental anatomically-constrained studies. Prior literature has recognized the power of functional alignment for individual differences studies[10,15,20,47], but it has remained underutilized in the developmental literature[8,17]. Recent work has recognized the need for massive numbers of subjects to reliably associate brain phenotypes with behavior, specifically in developmental cohorts[16]. We show that hyperalignment and connectome granularity analyses are powerful tools for understanding these individual differences, without the need for thousands of individuals and data points for model cross-validation – our hyperalignment model was learned on 200 subjects and tested entirely on resting-state data, with less than 20 minutes per subject. Further, it was trained and tested on independent subjects to assure that increased reliability was driven by generalizable, shared signals rather than overfitting to subject-specific signals. Though statistically significant, our predictions accounted for relatively low variance in behavioral measures relative to similar studies in adults[6,14,15]. Task-based functional connectivity is often more stable and predictive of behavior than RSFC among adults[13,15], but this is only with a sufficient amount of high-quality task data, which is known to be difficult to collect in children[35,48]. Individual differences in RSFC appear to be reliable in the ABCD dataset[17], whereas the task fMRI has known reliability limitations[13]. Previous studies have shown that both the ABCD task and resting whole-brain coarse FC can predict individual cognitive measures such as the toolbox tasks[9], with lower accuracy for the tasks comprising the learning/memory component than the general cognitive ability.

With the substantial twin cohort, behavioral testing, and longitudinal neuroimaging data included in ABCD, future work could investigate the connection between heritability and predictivity of functional connectivity over time, as the heritability of both neurocognitive measures and

neuroimaging-based phenotypes increase with age[1,5,49,50] By breaking apart the pieces of the functional connectome into their coarse and fine structures, we can show how these scales snap together like LEGO pieces to scaffold and instantiate reliable idiosyncrasies in brain and behavior during development.

Materials and methods

Participants

We considered data from the 11,875 children included in the Adolescent Brain Cognitive Development (ABCD) Study® [26], data release 2.0.1. The ABCD Study is a longitudinal study with 21 sites around the United States and aims to characterize cognitive and neural development with measures of neurocognition, physical and mental health, social and emotional function, and culture and environment. The ABCD Study obtained centralized institutional review board (IRB) approval from the University of California, San Diego, and each site obtained local IRB approval. Ethical regulations were followed during data collection and analysis. Parents or caregivers provided written informed consent, and children gave written assent. Four leading twin research centers at the University of Minnesota, Virginia Commonwealth University, University of Colorado-Boulder, and Washington University in St. Louis comprise the ABCD Twin Hub. Each site enrolled approximately 200 same-sex monozygotic or dizygotic twin pairs as well as singletons[27]. Their inclusion in the ABCD study affords unique access to the causal interrelation between genetics, environment, brain function, and cognition during development[1,5].

The present study uses imaging and behavioral data from a subset of n=1,115 subjects from the original 11,875 subjects. Included subjects were enrolled in the University of Minnesota, Washington University in St. Louis, and University of Colorado-Boulder sites, which all use 3T

Siemens MRI scanners. We excluded Virginia Commonwealth University, the fourth Twin Site, as it uses a GE scanner, a potential confound in the current study[26]. ABCD study-wide exclusion criteria include a diagnosis of schizophrenia, moderate to severe autism spectrum disorder, intellectual disabilities, major and persistent neurological disorders, multiple sclerosis, sickle cell disease, seizure disorders like Lennox-Gastaut Syndrome, Dravet Syndrome, and Landau Kleffner Syndrome, or substance abuse disorders at time of recruitment. Subjects with mild autism spectrum diagnosis, history of epilepsy, traumatic brain injury, and MR incidental findings were excluded from the present analysis.

Resting state fMRI data collection

Structural and functional data from the three included sites were acquired using Siemens Prisma 3T scanners with a 32-channel head coil. Detailed acquisition parameters are previously described in the literature[26,51]. Scan sessions consisted of a high-resolution (1 mm^3) T1-weighted image, diffusion weighted images, T2-weighted spin echo images (1 mm^3), resting-state fMRI (rs-fMRI), and task-based fMRI. We utilized rs-fMRI solely in this study. rs-fMRI data were collected with an echo-planar imaging sequence with 2.4 mm voxels, TR = 800 ms, TE = 30 ms, and multiband slice acceleration factor = 6. Participants completed up to four runs of 5-minute resting state scans. Framewise integrated real-time MRI monitoring (FIRMM[52]) was used to monitor subject head motion during data collection, and scan operators may have stopped resting-state data collection after three runs if 12.5 min of low-motion resting-state data had been collected.

Additional exclusions were made based on poor structural scan quality (determined with curated data release 2.0.1 sheet *freesqc01.txt*) or low quality/high motion resting state fMRI (determined as a score of zero for *fsqc_qc* or greater than one for *fsqc_qu_motion, fsqc_qu_pialover, fsqc_qu_wmunder,* or *fsqc_qu_inhomohgeneity*), as reported in prior studies[18]. Participants with fewer than 900 TRs of rs-fMRI data passing these measures for Freesurfer reconstruction were also excluded. ABCD Data Release 2.0.1 used Freesurfer version 5.3 for quality control checks[51]. After filtering, we used resting state fMRI and behavioral data from 1,115 unique subjects (552 male), including 170 pairs of monozygotic (MZ) twins, 219 pairs of dizygotic (DZ) twins, and 337 singletons. All twin pairs were same-sex, and all subjects were between 9 and 10 years old. Included singletons were also balanced for ancestry, ethnicity, sex, and pubertal development with twins (Table S1).

Preprocessing

rs-fMRI data were downloaded via the DCAN Labs ABCD-BIDS Community Collection (Fezco 2021) (NDA Collection 3165). This is a regularly updated dataset of ABCD Brain Imaging Data Structure (BIDS)[53] version 1.2.0 pipeline inputs and derivatives, using source data from the ABCD Study participants baseline year 1 arm 1 DICOM imaging data that passed initial acquisition quality control from the ABCD Data Analysis and Informatics Center (DAIC) [51] and retrieved from the NIMH Data Archive (NDA) share of ABCD fast-track data (NDA Collection 2573). DICOMs were converted to BIDS input data using Dcm2Bids[54] (make sure this is the zenodo), which reorganizes NiftiImages produced with dcm2niix (Xiangrui Li Et al 2016). Raw images were preprocessed using the the DCAN Labs ABCD-BIDS MRI processing pipeline[55] (for details, see github.com/DCAN-Labs/abcd-hcp-pipeline; osf.io/89pyd/; Sturgeon et al.,

2021), which is based on the Human Connectome Project (HCP) Minimal Preprocessing Pipeline[56] with additional modifications specifically for the ABCD dataset and summarized below.

The first stage of the pipeline, PreFreeSurfer, performs brain extraction, alignment, and N4 bias field correction on the T1w and T2w images. The second stage, FreeSurfer[57,58], segments the resulting T1w images and identifies tissue boundaries to register to a FreeSurfer template and produces brain masks. The third stage, PostFreeSurfer, uses the brain masks to register T1w images to MNI space using ANTs symmetric image normalization method[59]. Surfaces are then transformed to standard space using spherical registration and converted to CIFTI format along with the standardized brain volumes. The fMRIVolume stage performs functional image distortion correction using reverse phase-encoded spin echo images to correct for local field inhomogeneities. Eta squared values are computed for each image to a participant-level average of all field maps, and the pair with the highest value (i.e., most representative of the average) was selected to avoid potential motion confounds. Finally, the fMRISurface stage performs 2-mm full-width half-max spatial smoothing.

DCAN BOLD Processing[60] is used to perform standard data processing. First, fMRI data are demeaned and detrended with respect to time. Covariates of no interest were regressed from the data, including mean white matter, cerebrospinal fluid, overall global signal, mean grayordinate timeseries, and 6-movement variables (X,Y,Z translation and roll, pitch, yaw rotation). Timeseries data are then band-pass filtered between 0.008 and 0.09 Hz using a 2nd order Butterworth filter. Data is then filtered for respiratory motion for the frequencies (18,582 to

25.726 breaths per minute) of the respiratory signal, which has been shown to improve the stability of framewise displacement (FD) estimates[61]. "Bad" frames, where motion exceeds FD of 0.3 mm, are removed when demeaning and detrending such that denoising betas are only calculated for "good" frames. For the band-pass filtering, interpolation is used to replace those frames, so that pre-processing of the timeseries only includes "good" data but avoids aliasing due to missing timepoints. Finally, the filtered timeseries are normalized and concatenated across runs. The derivatives used in this analysis are *ses-baselineYear1Arm1_task-rest_bold_desc-filtered_timeseries.dtseries.nii.

Connectivity hyperalignment

We used connectivity hyperalignment[19] to functionally-align fine-scale connectivity information across subjects. Given the small quantity (1480 ± 142 TRs; mean±std) of resting state fMRI data available per subject, we chose to train the hyperalignment model common space using a cohort of 200 subjects who were then excluded from further analysis. These 200 training subjects were singletons enrolled at one of the three included sites and were matched with twin subjects on gender, pubertal development, age, and race/ethnicity (Table S1). The remaining 915 subjects (including the 389 twin pairs and 137 singletons) were used for subsequent analyses. Crucially, the hyperalignment model space never saw data from any subjects included in analyses during training.

We followed the same connectivity hyperalignment procedure for whole-cortex parcellation data as in our previous study[62]. We used the average timeseries for each of the 360 regions in the Glasser cortical parcellation[40] as connectivity targets and the vertices in each parcel as

connectivity seeds. For each parcel we computed a fine-scale connectivity matrix as the correlation between each of the vertices within the parcel and the average regional timeseries of the other 359 regions in the parcellation. For example, for a parcel with 430 vertices, its fine-scale connectivity matrix would be a matrix of dimensions 430 by 359 correlation coefficients, whereas its coarse-scale connectivity profile would be a vector of 359 correlation coefficients (Figure 1B).

For each region[20], we trained a separate high-dimensional common model space based on the fine-scale functional connectomes of the 200 training subjects. The dimensionality of the model space is equal to the number of vertices, but the model dimensions correspond to shared functional connectivity properties across individuals instead of anatomical locations[10]. After the model dimensions were learned, we discarded training subjects' data from downstream analyses. We derived invertible transformation matrices for the remaining subjects' connectomes into the model space to map vertex timeseries from the anatomically-defined dimensions into the functionally-defined dimensions.

Functional connectivity profiles

After aligning the test data into a common functional space, we used functional connectivity profiles to summarize a brain region's correlation with the rest of the cortex. We defined fine-scale functional connectivity profiles as above, as the correlation between the timeseries of all 59,412 vertices in the cortex with the average timeseries of each parcel, resulting in a matrix of 59,412 by 360 correlation coefficients per subject. We also defined coarse-scale functional connectivity profiles as the correlation between the average timeseries for all pairs of parcels,

resulting in a matrix of 360 by 360 correlation coefficients per subject (Figure 1B). The fine-scale and coarse-scale connectomes were computed on data pre- and post-hyperalignment for each subject to evaluate the effect of functional alignment and connectome granularity on heritability, reliability, and predictivity.

Reliability

Given the high levels of noise and low reliability associated with developmental neuroimaging data[35,48,63–65] as well as smaller (vertex-resolution) connectivity seeds[11], we used hyperalignment to improve the reliability of individual differences in our data. That is, by finding a space that aligns patterns of functional connectivity across subjects (within anatomically constrained parcels), we correct more thoroughly for anatomical variability and improve access to reliable individual differences [10,47] We calculated the reliability of functional connectomes before and after hyperalignment as follows. For 526 unrelated subjects, we computed fine-scale functional connectomes from split-half timeseries (742 ± 71 TRs). We derived transformation matrices to rotate these connectomes into the common space separately, then aligned the split timeseries data using those transformations. We then computed functional connectivity profiles, as explained above, for each half separately. For each parcel at the fine and coarse scale separately, we used the vectorized functional connectivity profiles before and after hyperalignment and computed individual differences matrices (IDM) for each data split. These are subject-by-subject pairwise dissimilarity matrices, where each value in the matrix is the correlation distance (1 - Pearson's r) between two subjects' regional connectivity profiles. After computing IDMs, we took the upper triangle of the IDM and correlated them (Pearson's r) to measure the reliability of the individual differences in the functional connectomes across the split halves[39]. This metric reflects the

reliability of the idiosyncrasies in a subject's functional connectomes, where subjects are more similar to themselves across split halves than they are to any other subject. We used a Mantel test[66,67] to perform statistical tests on IDMs with 10,000 permutations.

Multidimensional heritability estimation

Functional connectomes at vertex-granularity are an inherently high-dimensional phenotype; when dimensionality of the phenotype is collapsed, the reliability of individual differences decreases[39]. To offer greater statistical power in analyzing the heritability of this high-dimensional phenotype, we used a multidimensional estimate of heritability [32,68] to summarize the degree to which functional connectivity profiles for each parcel are under genetic control. We also investigated whether the alignment and granularity of the connectomes impact their heritability, which would indicate that the information highlighted by that type of connectome calculation is differentially impacted by genetics. Genetic kinship was estimated with SOLAR Kinship2[69].

Neurocognition PC prediction analysis

Neurocognition principal components (neurocog PCs)[45] were derived from the neurocognitive battery included in the ABCD study. The neurocognitive battery includes the NIH Toolbox cognition measures covering episodic memory, executive function, attention, working memory, processing speed, and language abilities. The neurocog PCs were derived with a Bayesian Probabilistic Principal Components Analysis, which revealed a three-component solution. The three components roughly corresponded to general cognitive ability, executive function, and learning/memory. Since the NIH Toolbox tasks that canonically measure executive function did

not load onto the executive function component in this solution, we excluded this component from our analyses, instead focusing on general cognitive ability and learning/memory. Tasks loading onto the general cognitive ability component include Toolbox Picture Vocabulary, Toolbox Oral Reading test, List Sort Working Memory task, and Little Man task. Tasks loading onto the learning/memory component include the Toolbox Picture Sequence Memory task, the RAVLT total number correct, and the List Sort Working Memory task. Heritability of composite scores were estimated with SOLAR Polygenic[69] including sex, age, ethnicity, and site as covariates (Figure S1A), as well as with Falconer's Formula[70] (Figure S1B).

We predicted loadings onto the neurocognition principal components based on functional connectivity from our cohort of 526 unrelated subjects using a principal component ridge regression adapted from our previous study[62]. First, we used principal components analysis (PCA) to train principal components (PCs) to capture the main orthogonal dimensions along which individuals' connectivity profiles differ from one another. We then trained a ridge regression model to predict learning and memory scores from these PC scores, and tested the PCA and ridge regression models by predicting the learning and memory score of the held-out subjects. Model parameters (number of PCs and regularization parameter α) were chosen with nested cross-validation using three sub-folds. Candidate model parameters were distributed evenly on a logarithmic scale, from 10 to 320 PCs and no PCs (no dimensionality reduction), and α chosen from 121 values between 10^{-20} to 10^{40}. Models were evaluated using the cross-validated coefficient of determination R^2 , which shows the percent of variance in learning and memory scores accounted for by the prediction models. To assess statistical significance of model

performance against chance, we used permutation testing with 1000 iterations of shuffling the behavioral scores.

Data availability

The ABCD study is longitudinal, so the data repository changes over time and can be found here: https://nda.nih.gov/abcd. In the current study, we used the ABCD data release 2.0.1, downloaded via ABCD-BIDS Community Collection[71] NDA Collection 3165.

Code availability

ABCD data preprocessing code can be found here: https://github.com/DCAN-Labs/abcd-hcp-pipeline. ABCD data processing code can be found here: https://github.com/DCAN-Labs/dcan_bold_processing. Code for running the multiscale heritability analysis can be found here: https://github.com/kevmanderson/h2_multi. Code for running the nested PCA ridge regression was based off: https://github.com/feilong/IDM_pred. All analysis code specific to this study will be released upon publication.

Acknowledgements

This project was supported by the National Science Foundation Graduate Research Fellowship Award # 2139841 to Erica L. Busch.

Data used in the preparation of this article were obtained from the Adolescent Brain Cognitive Development (ABCD) Study (https://abcdstudy.org), held in the NIMH Data Archive (NDA). This is a multisite, longitudinal study designed to recruit more than 10,000 children age 9-10 and follow them over 10 years into early adulthood. The ABCD Study is supported by the National

Institutes of Health and additional federal partners under award numbers U01DA041048, U01DA050989, U01DA051016, U01DA041022, U01DA051018, U01DA051037, U01DA050987, U01DA041174, U01DA041106, U01DA041117, U01DA041028, U01DA041134, U01DA050988, U01DA051039, U01DA041156, U01DA041025, U01DA041120, U01DA051038, U01DA041148, U01DA041093, U01DA041089, U24DA041123, U24DA041147. A full list of supporters is available at https://abcdstudy.org/federal-partners.html. A listing of participating sites and a complete listing of the study investigators can be found at https://abcdstudy.org/consortium_members/. ABCD consortium investigators designed and implemented the study and/or provided data but did not necessarily participate in analysis or writing of this report. This manuscript reflects the views of the authors and may not reflect the opinions or views of the NIH or ABCD consortium investigators.

This research also benefited from the ABCD Workshop on Brain Development and Mental Health, supported by the National Institute of Mental Health of the National Institutes of Health under Award Number R25MH120869 and by UG3-DA045251 from the National Institute of Drug Abuse.

Supplemental tables and figures

Table S1: Cohort Breakdown

	Total Included	Monozygotic Pairs	Dizygotic Pairs	Unrelated Test	Unrelated Train
Total	1,115	170	219	526	200
Site 20	387	75	86	184	60
Site 21	371	34	81	166	90
Site 22	357	75	68	176	60
Age (mo) (*interview_age*)	121.6	122.5	122.0	121.6	120.7
% Female (*gender*)	50%	52%	50%	50%	50%
Ancestry: African (*AFR*)	0.127	0.092	0.118	0.113	0.204
Ancestry: European (*EUR*)	0.805	0.825	0.826	0.814	0.733
Ancestry: East Asian (*EAS*)	0.020	0.016	0.016	0.021	0.025
Ancestry: (*AMR*)	0.049	0.067	0.040	0.052	0.038
Ethnicity (*race_ethnicity*)	1.667	1.659	1.63	1.73	1.58

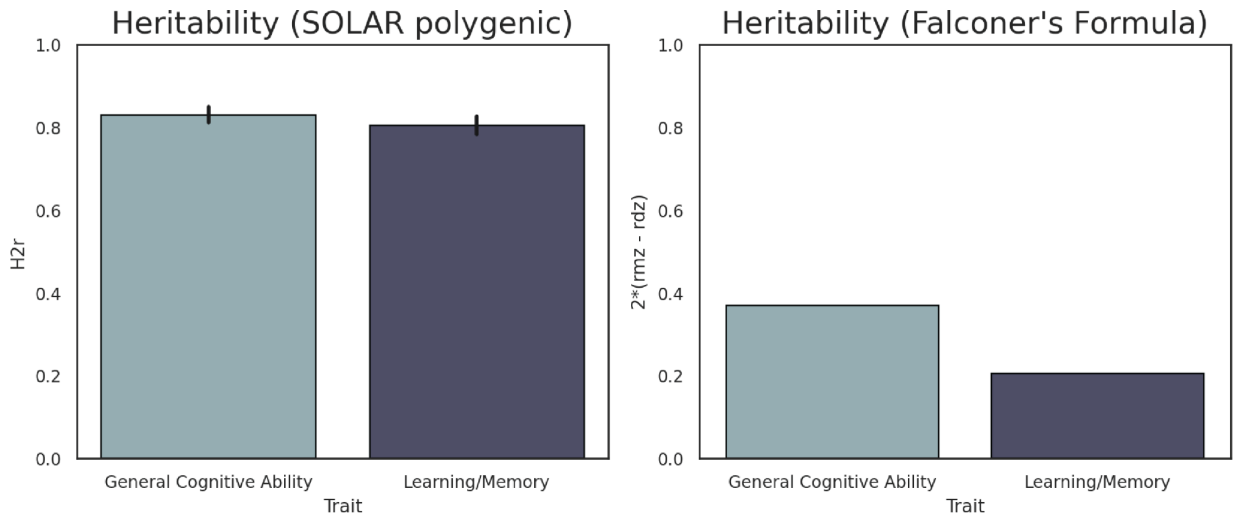

Figure S1: Heritability of general cognitive ability and learning/memory loadings.
Left: Heritability estimated with SOLAR Polygenic (covariate tested: site, age, sex, and ethnicity), presented as H2r and error bars representing standard error.
Right: Heritability estimated with Falconer's formula (2 times intraclass correlation coefficients for monozygotic twins – dizygotic twins).

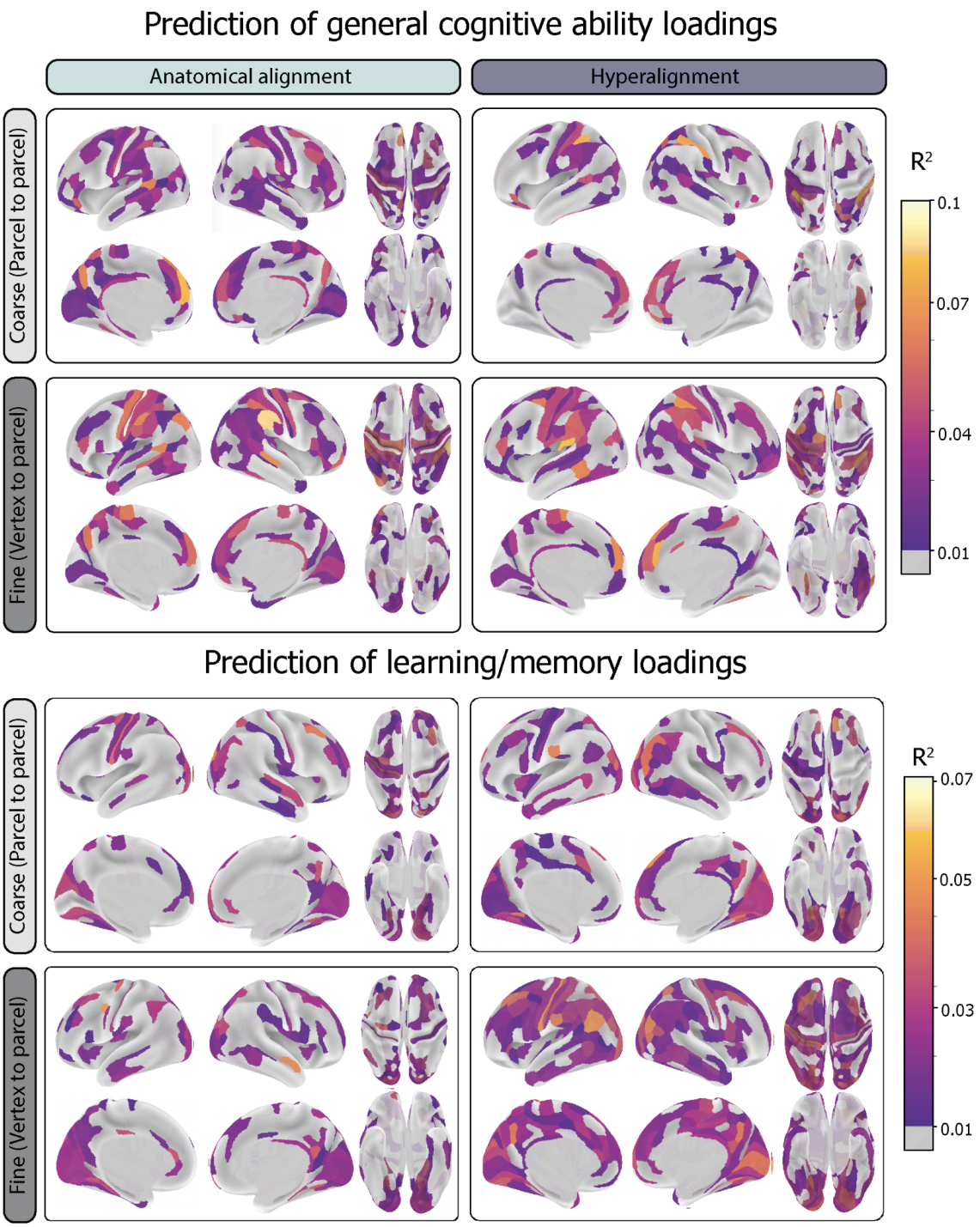

Figure S2: Prediction of neurocognition displayed on cortical surface.

Prediction of individual differences in the general cognitive ability component (top) and the learning/memory component (bottom). R^2 values displayed for each parcel and significance assessed with 1000 permutations. Nonsignificant R^2 values ($p>0.01$) displayed in gray.

References

1. Blokland, G. A. M., de Zubicaray, G. I., McMahon, K. L. & Wright, M. J. Genetic and Environmental Influences on Neuroimaging Phenotypes: A Meta-Analytical Perspective on Twin Imaging Studies. *Twin Res. Hum. Genet. Off. J. Int. Soc. Twin Stud.* **15**, 351–371 (2012).
2. Brouwer, R. M. *et al.* Heritability of brain volume change and its relation to intelligence. *NeuroImage* **100**, 676–683 (2014).
3. Elliott, L. T. *et al.* Genome-wide association studies of brain imaging phenotypes in UK Biobank. *Nature* **562**, 210–216 (2018).
4. Hulshoff Pol, H. E. *et al.* Genetic Contributions to Human Brain Morphology and Intelligence. *J. Neurosci.* **26**, 10235–10242 (2006).
5. Jansen, A. G., Mous, S. E., White, T., Posthuma, D. & Polderman, T. J. What twin studies tell us about the heritability of brain development, morphology, and function: a review. *Neuropsychol. Rev.* **25**, 27–46 (2015).
6. Dubois, J., Galdi, P., Paul, L. K. & Adolphs, R. A distributed brain network predicts general intelligence from resting-state human neuroimaging data. *Philos. Trans. R. Soc. B Biol. Sci.* **373**, 20170284 (2018).
7. Finn, E. S. & Rosenberg, M. D. Beyond fingerprinting: Choosing predictive connectomes over reliable connectomes. *NeuroImage* **239**, 118254 (2021).
8. Sripada, C. *et al.* Prediction of neurocognition in youth from resting state fMRI. *Mol. Psychiatry* **25**, 3413–3421 (2020).
9. Chen, J. *et al.* Shared and unique brain network features predict cognitive, personality, and mental health scores in the ABCD study. *Nat. Commun.* **13**, 2217 (2022).

10. Haxby, J. V., Guntupalli, J. S., Nastase, S. A. & Feilong, M. Hyperalignment: Modeling shared information encoded in idiosyncratic cortical topographies. *eLife* **9**,.
11. Haak, K. V., Marquand, A. F. & Beckmann, C. F. Connectopic mapping with resting-state fMRI. *NeuroImage* **170**, 83–94 (2018).
12. Lin, Q., Yoo, K., Shen, X., Constable, T. R. & Chun, M. M. Functional Connectivity during Encoding Predicts Individual Differences in Long-Term Memory. *J. Cogn. Neurosci.* **33**, 2279–2296 (2021).
13. Rosenberg, M. D. *et al.* A neuromarker of sustained attention from whole-brain functional connectivity. *Nat. Neurosci.* **19**, 165–171 (2016).
14. Finn, E. S. *et al.* Functional connectome fingerprinting: identifying individuals using patterns of brain connectivity. *Nat. Neurosci.* **18**, 1664–1671 (2015).
15. Feilong, M., Guntupalli, J. S. & Haxby, J. V. The neural basis of intelligence in fine-grained cortical topographies. *eLife* vol. 10 e64058 (2021).
16. Marek, S. *et al.* Reproducible brain-wide association studies require thousands of individuals. *Nature* **603**, 654–660 (2022).
17. Marek, S. *et al.* Identifying reproducible individual differences in childhood functional brain networks: An ABCD study. *Dev. Cogn. Neurosci.* **40**, (2019).
18. Rosenberg, M. D. *et al.* Behavioral and Neural Signatures of Working Memory in Childhood. *J. Neurosci.* **40**, 5090–5104 (2020).
19. Guntupalli, J. S., Feilong, M. & Haxby, J. V. A computational model of shared fine-scale structure in the human connectome. *PLOS Comput. Biol.* **14**, e1006120 (2018).
20. Haxby, J. V. *et al.* A Common, High-Dimensional Model of the Representational Space in Human Ventral Temporal Cortex. *Neuron* **72**, 404–416 (2011).

21. Glahn, D. C. *et al.* Genetic control over the resting brain. *Proc. Natl. Acad. Sci. U. S. A.* **107**, 1223–1228 (2010).

22. Miranda-Dominguez, O. *et al.* Heritability of the human connectome: A connectotyping study. *Network Neuroscience* vol. 02 175–199 (2018).

23. Yang, Z. *et al.* Genetic and Environmental Contributions to Functional Connectivity Architecture of the Human Brain. *Cereb. Cortex N. Y. N 1991* **26**, 2341–2352 (2016).

24. Cui, Z. *et al.* Individual Variation in Functional Topography of Association Networks in Youth. *Neuron* vol. 106 340-353.e8 (2020).

25. Dosenbach, N. U. F. *et al.* Prediction of Individual Brain Maturity Using fMRI. *Science* **329**, 1358–1361 (2010).

26. Casey, B. J. *et al.* The Adolescent Brain Cognitive Development (ABCD) study: Imaging acquisition across 21 sites. *Dev Cogn Neurosci* vol. 32 43–54 (2018).

27. Iacono, W. G. *et al.* The utility of twins in developmental cognitive neuroscience research: How twins strengthen the ABCD research design. *Dev. Cogn. Neurosci.* **32**, 30–42 (2017).

28. Peper, J. S. *et al.* Heritability of regional and global brain structure at the onset of puberty: A magnetic resonance imaging study in 9-year-old twin pairs. *Hum. Brain Mapp.* **30**, 2184–2196 (2009).

29. Thompson, P. M. *et al.* Genetic influences on brain structure. *Nat. Neurosci.* **4**, 1253–1258 (2001).

30. Colclough, G. L. *et al.* The heritability of multi-modal connectivity in human brain activity. *eLife* vol. 6 e20178 (2017).

31. Barber, A. D., Hegarty, C. E., Lindquist, M. & Karlsgodt, K. H. Heritability of Functional Connectivity in Resting State: Assessment of the Dynamic Mean, Dynamic Variance, and

Static Connectivity across Networks. *Cereb. Cortex N. Y. NY* **31**, 2834–2844 (2021).

32. Anderson, K. M. *et al.* Heritability of individualized cortical network topography. *Proc. Natl. Acad. Sci.* **118**, e2016271118 (2021).
33. Ge, T., Holmes, A. J., Buckner, R. L., Smoller, J. W. & Sabuncu, M. R. Heritability analysis with repeat measurements and its application to resting-state functional connectivity. *Proc. Natl. Acad. Sci.* **114**, 5521–5526 (2017).
34. Fu, Y. *et al.* Genetic influences on resting-state functional networks: A twin study. *Hum. Brain Mapp.* **36**, 3959–3972 (2015).
35. Kennedy, J. T. *et al.* Reliability and Stability Challenges in ABCD Task fMRI Data. *bioRxiv* doi:https://doi.org/10.1101/2021.10.08.463750.
36. Schmitt, J. E. *et al.* The dynamic role of genetics on cortical patterning during childhood and adolescence. *Proc. Natl. Acad. Sci.* **111**, 6774–6779 (2014).
37. Lenroot, R. K. *et al.* Differences in genetic and environmental influences on the human cerebral cortex associated with development during childhood and adolescence. *Hum. Brain Mapp.* **30**, 163–174 (2009).
38. Achterberg, M. *et al.* Distinctive heritability patterns of subcortical-prefrontal cortex resting state connectivity in childhood: A twin study. *NeuroImage* **175**, 138–149 (2018).
39. Feilong, M., Nastase, S. A., Guntupalli, J. S. & Haxby, J. V. Reliable individual differences in fine-grained cortical functional architecture. *NeuroImage* vol. 183 375–386 (2018).
40. Glasser, M. F. *et al.* A multi-modal parcellation of human cerebral cortex. *Nature* vol. 536 171–178 (2016).
41. Yates, T. S., Ellis, C. T. & Turk-Browne, N. B. Emergence and organization of adult brain function throughout child development. *NeuroImage* **226**, 117606 (2021).

42. Noble, S. *et al.* Influences on the Test–Retest Reliability of Functional Connectivity MRI and its Relationship with Behavioral Utility. *Cereb. Cortex* **27**, 5415–5429 (2017).

43. Plomin, R. & Deary, I. J. Genetics and intelligence differences: five special findings. *Mol. Psychiatry* **20**, 98–108 (2015).

44. Mollon, J. *et al.* Genetic influence on cognitive development between childhood and adulthood. *Mol. Psychiatry* **26**, 656–665 (2021).

45. Thompson, W. K. *et al.* The structure of cognition in 9 and 10 year-old children and associations with problem behaviors: Findings from the ABCD study's baseline neurocognitive battery. *Dev. Cogn. Neurosci.* **36**, 100606 (2019).

46. Johnson, M. H. Interactive Specialization: A domain-general framework for human functional brain development? *Dev. Cogn. Neurosci.* **1**, 7–21 (2011).

47. Dubois, J. & Adolphs, R. Building a Science of Individual Differences from fMRI. *Trends Cogn Sci* vol. 20 425–443 (2016).

48. Satterthwaite, T. D. *et al.* Impact of in-scanner head motion on multiple measures of functional connectivity: Relevance for studies of neurodevelopment in youth. *NeuroImage* **60**, 623–632 (2012).

49. Haworth, C. M. A. *et al.* The heritability of general cognitive ability increases linearly from childhood to young adulthood. *Mol. Psychiatry* **15**, 1112–1120 (2010).

50. Briley, D. A. & Tucker-Drob, E. M. Explaining the Increasing Heritability of Cognitive Ability Across Development: A Meta-Analysis of Longitudinal Twin and Adoption Studies. *Psychol. Sci.* **24**, 1704–1713 (2013).

51. Hagler, D. J. *et al.* Image processing and analysis methods for the Adolescent Brain Cognitive Development Study. *NeuroImage* **202**, 116091 (2019).

52. Dosenbach, N. U. *et al.* Real-time motion analytics during brain MRI improve data quality and reduce costs. *Neuroimage* **161**, 80–93 (2017).

53. Gorgolewski, K. J. *et al.* The brain imaging data structure, a format for organizing and describing outputs of neuroimaging experiments. *Sci. Data* **3**, 160044 (2016).

54. *dcm2bids*. (UNF, 2022).

55. dsturge, Earl, E. & kathy-snider. *DCAN-Labs/abcd-hcp-pipeline: release v0.0.0*. (Zenodo, 2019). doi:10.5281/zenodo.2587210.

56. Glasser, M. F. *et al.* The minimal preprocessing pipelines for the Human Connectome Project. *NeuroImage* **80**, 105–124 (2013).

57. Dale, A. M., Fischl, B. & Sereno, M. I. Cortical surface-based analysis. I. Segmentation and surface reconstruction. *NeuroImage* **9**, 179–194 (1999).

58. Fischl, B. FreeSurfer. *NeuroImage* **62**, 774–781 (2012).

59. Avants, B. B. *et al.* A reproducible evaluation of ANTs similarity metric performance in brain image registration. *NeuroImage* **54**, 2033–2044 (2011).

60. *dcan signal processing*. (Developmental Cognition and Neuroimaging Labs, 2022).

61. Fair, D. A. *et al.* Correction of respiratory artifacts in MRI head motion estimates. *NeuroImage* **208**, 116400 (2020).

62. Feilong, M., Guntupalli, J. S. & Haxby, J. V. *The neural basis of intelligence in fine-grained cortical topographies*. http://biorxiv.org/lookup/doi/10.1101/2020.06.06.138099 (2020).

63. Birn, R. M. *et al.* The effect of scan length on the reliability of resting-state fMRI connectivity estimates. *NeuroImage* **83**, 550–558 (2013).

64. Power, J. D., Barnes, K. A., Snyder, A. Z., Schlaggar, B. L. & Petersen, S. E. Spurious but systematic correlations in functional connectivity MRI networks arise from subject motion.

NeuroImage **59**, 2142–2154 (2012).

65. Fair, D. *et al.* Distinct neural signatures detected for ADHD subtypes after controlling for micro-movements in resting state functional connectivity MRI data. *Front. Syst. Neurosci.* **6**, (2013).
66. Mantel, N. Ranking Procedures for Arbitrarily Restricted Observation. *Biometrics* **23**, 65–78 (1967).
67. Carr, J. *mantel*. (2021).
68. Ge, T. *et al.* Multidimensional heritability analysis of neuroanatomical shape. *Nat. Commun.* **7**, 13291 (2016).
69. Almasy, L. & Blangero, J. Multipoint quantitative-trait linkage analysis in general pedigrees. *Am. J. Hum. Genet.* **62**, 1198–1211 (1998).
70. Falconer, D. S. *Introduction to quantitative genetics*. (Pearson Education India, 1996).
71. Feczko, E. *et al.* Adolescent Brain Cognitive Development (ABCD) Community MRI Collection and Utilities. 2021.07.09.451638 (2021) doi:10.1101/2021.07.09.451638.